Journal Pre-Proof


Enhanced photoreductive degradation of perfluorooctanesulfonate by UV irradiation in the presence of ethylenediaminetetraacetic acid

Pengfei Gu, Chaojie Zhang, Zhuyu Sun, Haozhen Zhang, Qi Zhou, Sijie Lin, Jinyu Rong, Michael R. Hoffmann

PII: S1385-8947(19)31741-3
DOI: https://doi.org/10.1016/j.cej.2019.122338
Reference: CEJ 122338

To appear in: *Chemical Engineering Journal*

Received Date: 12 April 2019
Revised Date: 23 July 2019
Accepted Date: 25 July 2019

Please cite this article as: P. Gu, C. Zhang, Z. Sun, H. Zhang, Q. Zhou, S. Lin, J. Rong, M.R. Hoffmann, Enhanced photoreductive degradation of perfluorooctanesulfonate by UV irradiation in the presence of ethylenediaminetetraacetic acid, *Chemical Engineering Journal* (2019), doi: https://doi.org/10.1016/j.cej.2019.122338

# Enhanced photoreductive degradation of perfluorooctanesulfonate by UV irradiation in the presence of ethylenediaminetetraacetic acid

Pengfei Gu[a, b], Chaojie Zhang*[, a, b], Zhuyu Sun[a, b], Haozhen Zhang[a, b], Qi Zhou[a, b], Sijie Lin[a, b], Jinyu Rong[a, b] and Michael R. Hoffmann[c]

[a] State Key Laboratory of Pollution Control and Resources Reuse, College of Environmental Science and Engineering, Tongji University, Shanghai 200092, China

[b] Shanghai Institute of Pollution Control and Ecological Security, Shanghai 200092, China

[c] Linde-Robinson Laboratories, California Institute of Technology, Pasadena, California 91125, United States

* Corresponding author. Tel: +86 21 65981831; fax: +86 21 65983869;

E-mail address: myrazh@tongji.edu.cn

**Abstract**

Perfluorooctanesulfonate (PFOS) is a persistent organic pollutant (POP) that is globally distributed. Hydrated electrons ($e_{aq}^-$) are known to effectively initiate the decomposition of PFOS. In this study, we explore an alternative photolytic approach employing aquated electrons, $e_{aq}^-$ in the presence of ethylenediaminetetraacetic acid (EDTA) in order to enhance the photo-induced degradation of PFOS. EDTA, in this case, serves primarily as a hydroxyl radical scavenger, which inhibits the recombination of $e_{aq}^-$ with ·OH resulting in an increased average photolytic lifetime for $e_{aq}^-$. The net effect is to enhance the degradation of PFOS. UV/EDTA irradiation is shown to increase the overall decomposition percentages of PFOS. The empirical pseudo first-order rate constant for the loss of PFOS is 0.113 $h^{-1}$. In addition, we used laser flash photolysis kinetics to show that the $e_{aq}^-$ is the dominant species responsible for the decomposition of PFOS. EDTA also allows for the photolytically-produced hydrated electrons to be used in the presence of air over a wide range of pH. Furthermore, perfluoroalkyl sulfonates with longer chain lengths have higher overall decomposition percentages and increased defluorination percentages. The observed kinetic enhancements appear to be due primarily to the impact of the amine and methylene groups of EDTA with respect of hydroxyl radical scavenging.

## 1. Introduction

Over the past 60 years, perfluorinated compounds (PFCs) such as perfluorooctane sulfonate (PFOS) and perfluorooctanic acid (PFOA), have been widely used in industrial, medical and domestic applications due to their stable physical and chemical properties [1-3]. However, PFOS is persistent in the environment, bioaccumulates, and is widely distributed globally [3, 4]. PFOS is recalcitrant to conventional chemical and thermal degradation primarily due to the high electronegativity of the fluorine (i.e., $E^0(F/F^-)$ = 3.6V) [5] and the strength of the carbon-fluorine (C-F) bonds (i.e., bond dissociation energy (BDE) ≥ 445 kcal/mol) [6]. PFOS is known to be neurotoxic and hepatotoxic to humans and animals [7, 8]. PFOS has been classified as a Persistent Organic Pollutants (POP) by the Stockholm Convention in May 2009 [9].

Hydrated electrons ($e_{aq}^-$) are powerful reducing agents that have been shown to be effective for degrading PFOS. Hydrated electrons can be generated using electron beam bombardment [10], gamma-ray radiation [11], and by UV photolysis of sulfite [12], iodide [13] and 3-indole acetic acid [14, 15]. Electron beam and gamma-ray radiation has been used to decompose PFOS, considering the fixed cost such as high equipment cost, interest and depreciation [16], the cost is too high for an economical engineering treatment method. A catalyst-free PFOS photodecomposition method that requires high temperatures (e.g., 100 $^oC$) and alkaline conditions (pH =11.8) has been reported to exhibit great performance in PFOS decomposition [17]. But high temperature and strong alkaline conditions would be bottleneck of the application of this process. UV photolysis of sulfite [12, 18] or iodide [13] produces a sufficient level of $e_{aq}^-$, being

efficient in PFOS decomposition. However, these techniques do not function well under acidic and circum-neutral pH for inducing PFOS decomposition. Besides, due to the rapid second-order reaction between $e_{aq}^-$ and $O_2$ (**Eq. 1**, $k_1 = 1.9\times10^{10}$ $M^{-1}\cdot s^{-1}$) [19], PFOS decomposition efficiencies induced by $e_{aq}^-$ are reduced in the presence of dissolved oxygen. Thus, $e_{aq}^-$-mediated photo-reductive degradation normally requires strict anoxic conditions [20, 21]. In addition, the formation of undesirable reaction byproducts during PFOS decomposition may occur in some photochemical processes. For example, in UV/KI process, secondary reaction byproducts and intermediates were formed including iodine, polyiodide, and iodate, which could have undesirable impact on human health or on the health of the aquatic environment due to their genotoxicity and carcinogenicity [22, 23]. Alternative photo-reductive systems such as the UV/sulfite also have resulted in the formation of undesirable by-products. Sulfite alone has been shown to have reproductive toxicity and peripheral organ toxicity [24].

UV irradiation or ionizing radiation such as gamma and electron beam irradiation of water generates $e_{aq}^-$, hydroxyl radicals (·OH), $H_3O^+$ and several other species of much lower concentrations (**Eq. 2-3**) [25, 26]. However, recombination of $e_{aq}^-$ with ·OH (**Eq. 4-6**) reduces the effectives of the process. Thus, only a small fraction of $e_{aq}^-$ escapes into the bulk solution to initiate reductive electron transfer to target substrates [19]. Consequently, we have proposed an alternative approach to enhance the production of $e_{aq}^-$ by inhibiting its recombination with susceptible reductants added to the reaction solution.

$$e_{aq}^- + O_2 \rightarrow O_2^{\cdot -} \qquad (1) \qquad H_2O \xrightarrow{h\nu} e_{aq}^- + \cdot OH + H\cdot + H_3O^+ \qquad (2)$$

$$H_2O \xrightarrow{\gamma \text{ or } EB} e_{aq}^- + \cdot OH + H\cdot + H_3O^+ + H_2 + H_2O_2 \quad (3)$$

$$e_{aq}^- + \cdot OH \rightarrow OH^- \quad (4)$$

$$e_{aq}^- + H\cdot \rightarrow H_2 + OH^- \quad (5)$$

$$e_{aq}^- + H_3O^+ \rightarrow H\cdot + H_2O \quad (6)$$

Aminopolycarboxylic acids such as ethylenediaminetetraacetic acid (EDTA), nitrilotriacetic acid (NTA), are known to react readily with ·OH [27, 28]. A previous study demonstrated that UV photolysis of NTA was efficient in PFOS decomposition, even in open air condition [27]. Thus, given the potential use of ETDA as a hydroxyl radical scavenger, we herein report on: (1) the efficiency of UV/EDTA photolysis for PFOS decomposition, (2) determine the decomposition kinetics of PFOS over a broad range of pH and solution composition, (3) report on the formation of reaction intermediates and to propose a self-consistent mechanism for PFOS degradation taking place during UV/EDTA photolysis based on laser flash photolysis probing of key reaction intermediates.

## 2. Materials and methods

### 2.1 Chemicals and materials

Perfluorooctanoic acid (PFOA, ≥90%), perfluoropentanoic acid (PFPeA, ≥94%), perfluorohexanoic acid (PFHxA, ≥97%) and perfluorohexanesulfonic acid potassium salt (PFHxS, ≥98%) were obtained from Fluka (Swizerland). Perfluorooctanesulfonic acid (PFOS) was purchased from ABCRGmbH & Co. KG, Karlsruhe (Germany). Pentafluoropropionic acid (PFPrA, 99%), perfluorobutyric acid (PFBA, 99%), perfluoroheptanoic acid (PFHpA, 99%) and perfluoro-1-butanesulfonic acid (PFBS,

98%) were purchased from Sigma-Aldrich (USA). Perfluoro-n-[1,2,3,4-$^{13}C_4$]octanoic acid (MPFOA, >98%) and sodium perfluoro-1-[1,2,3,4-$^{13}C_4$]octanesulfonate (MPFOS, >99%) were purchased from Wellington Laboratories Inc. (Canada). Formic acid (96%) and acetic acid (99.7%) were obtained from TEDIA Co. (USA). Sodium fluoride (99.99%), EDTA, ammonium chloride, ammonium hydroxide, hydrochloric acid, potassium iodide, sodium sulphate anhydrous, AHMT (4-Amino-3-hydrazino-5-mercapto-1, 2, 4-triazole), HEDTA and TMEDA (≥98%) were purchased from Sinopharm Chemical Reagents (China). Deionized water was produced in the laboratory using a Milli-Q integral water purification system (Millipore, USA).

**2.2. Reductive decomposition**

The reductive decomposition of PFOS with hydrated electrons in anoxic aqueous solutions was performed in a stainless-steel cylindrical reactor with a 60 mm inner diameter equipped with a low- pressure mercury lamp (14W, λ=254 nm) (for details, see **Supplementary Material**, **Fig. S1**). A 720 mL solution of PFOS (0.01 mM) and EDTA (0-2 mM) was added to the reactor，and then stirred by a magnetic stirrer at 120rpm and irradiated internally with the mercury lamp. Before the reaction, the mixture was bubbled with highly purified nitrogen for 20 minutes in order to remove a large fraction of dissolved oxygen. The initial pH of the $N_2$-purged solution was adjusted with hydrochloric acid (HCl) and sodium hydroxide (NaOH). The reaction temperature was held constant at 25 ◦C with the circulating temperature controller.

The initial concentrations of PFOS and EDTA were 0.01 mM and 2.0 mM, respectively, while the initial pH was adjusted to 10.0. In order to determine the effect

of each variable, five control experiments were conducted. The first control experiment was conducted in the absence of EDTA under identical conditions. The second control experiment (i.e., direct photolysis) was carried out in the absence of EDTA and without adjusting solution pH. The third control experiment was a dark reaction under the same concentration conditions without illumination. The fourth control experiment was conducted with the addition of $K_2S_2O_8$ and without $N_2$ purging at solution pH of 3 [29]. The fifth control experiment was carried out under similar conditions in the presence of $N_2O$ in the absence of $N_2$.

At various time intervals, samples of the reaction mixture were collected and analyzed for $F^-$ using ion chromatography (IC) and high-performance liquid chromatography-tandem/mass spectrometry (HPLC/MS/MS). Before the analysis, all the samples were filtered through 0.22 μm nylon filter membranes.

### 2.3. Analytical methods

The concentrations of PFOS, PFOS-derived aqueous phase intermediate and EDTA were determined using high-performance liquid chromatography/tandem mass spectrometry (HPLC−MS/MS, TSQ™ Quantum Access™, Thermo Finnigan, San Jose, CA, USA). The HPLC system employed an Agilent ZORBAX Eclipse Plus C18 column (2.1 × 150 mm, 3.5 μm). A mixture of methanol and 2 mM ammonium acetate was used as the mobile phase. Detailed information is available in the **Supplementary Material**.

An Ion Chromatograph (Dionex, ICS-3000, Thermo Fisher Scientific, USA), which was equipped with a conductivity detector and a self-regenerating suppressor,

was used for the analysis of fluoride, sulfate, acetate, formate and nitrate. Detailed information is available in the **Supplementary Material**.

An AHMT method was used for formaldehyde quantification [30]. The concentration of ammonia was measured according to standard method [31]. Detailed information is available in the **Supplementary Material**.

### 2.4. Calculations

Decomposition percentage of PFOS was calculated as follows:

$$\text{Decomposition percentage} = \frac{c_F}{c_0} \times 100\% \qquad (7)$$

Defluorination percentage of PFOS was calculated as follows:

$$\text{Defluorination percentage} = \frac{c_F}{17 \times c_0} \times 100\% \qquad (8)$$

where $C_F^-$ is the concentration of fluoride ion (μM); $C_0$ is the initial concentration of PFOS (μM), and the factor 17 corresponds to the number of fluorine atoms15 in one PFOS molecule.

The mass balance of fluorine element (F) was calculated based on the concentrations of PFOS, F-containing intermediates and $F^-$. The recovery of fluorine element ($R_F$) is defined as follows:

$$R_F = \frac{(2n+1)\sum_1^6 C_{CF_3(CF_2)_nCOO^-} + (2n+1)\sum_3^7 C_{CF_3(CF_2)_nSO_3^-}}{C_0 \times 17} \qquad (9)$$

where, $(2n+1)\sum_1^6 C_{CF_3(CF_2)_nCOO^-}$ is the total fluorine element (F) concentration of PFCAs (C3 to C8) (mM) at the irradiation time t (h). $(2n+1)\sum_3^7 C_{CF_3(CF_2)_nSO_3^-}$ is the total fluorine element (F) concentration of PFSAs (C4, C6 and C8) (mM) at the irradiation time t (h). $C_0$ is the initial concentration of PFOS (mM) at the irradiation

time t (h).

### 2.5. Laser flash photolysis (LFP) experiments

Laser flash photolysis experiments were performed in order to detect transient species generated as a function of the intensity of the laser light. Excitation of the third harmonic of pterin (2-aminopteridin-4(3*H*)-one) was achieved and recorded on a Surelite I-10 Q-Switched Nd:YAG laser (6 ns FWHM, 10 mJ per pulse) at an excitation wavelength of 266 nm. The transient absorption spectra of aqueous solutions purged and saturated with $N_2$, were recorded with a LP980 laser flash photolysis apparatus linked to a 100 MHz Tektronix TDS3012C digital oscilloscope for signal acquisition. Signal analyses were performed using the L900 spectrometer software.

Transient species characterization after laser flash photolysis at $\lambda$ = 266 nm was followed over the wavelength range 350 nm and 780 nm and 10 nm intervals on a solution 50 mM EDTA in $N_2$-purged water.

### 2.6. Zebrafish embryo toxicity test

The AB wild-type adult zebrafish (Danio rerio) were maintained at 28 ± 0.5 ◦C on a 14 h:10 h light/dark cycle in a fish breeding circulatory system (Haisheng, Shanghai, China) and were fed twice daily with live brine shrimps (Artemia salina). Two pairs of male/female fish were placed in a single mating box separated by a divider 1 day prior to spawning. Spawning was triggered by removing the divider in the morning and the embryos were collected 2 h afterwards. Embryos washed with 0.5 ppm methylene blue solution were then transferred to Holtfreter's medium in a Petri-dish. Using a stereomicroscope (Olympus-SZ61, Olympus Ltd., Japan), healthy and fertilized

embryos at 4 h post fertilization (hpf) were selected and placed in Ubottom 96-well plates (Costar-3599, Corning, US), with one embryo per well. Each was then filled with 200 μL of series of the treatment samples as well as H-buffer as negative controls. Three replicates were carried out for each treatment, each using 12 embryos. The developmental status of the zebrafish embryos was observed at 24 h, 48 h, and 72 h. The toxicological endpoints included hatching interference, phenotypic abnormalities and mortality (necrosis of the embryos). All zebrafish related experiments were carried out in accordance with the Animal Ethics Committee at Tongji University, with protocol approved by the Animal Center of Tongji University (Protocol #TJLAC-018-020).

## 3. Results and discussion

### 3.1 Photo-reductive defluorination of PFOS

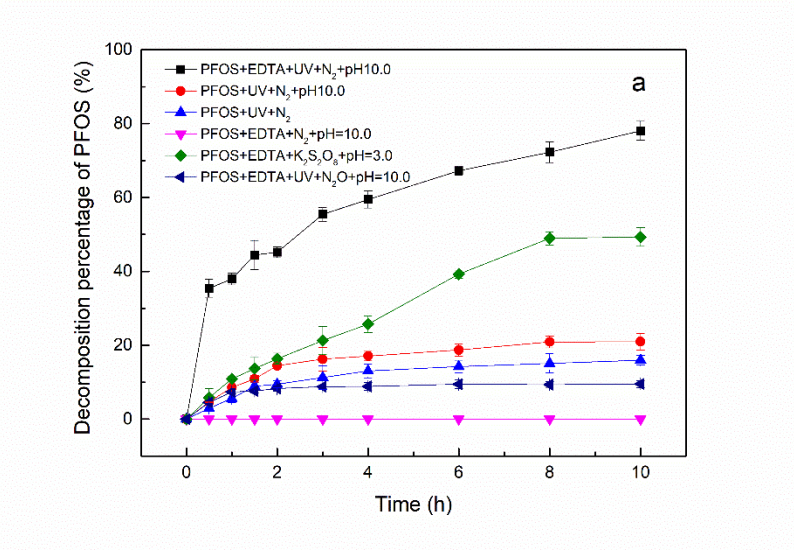

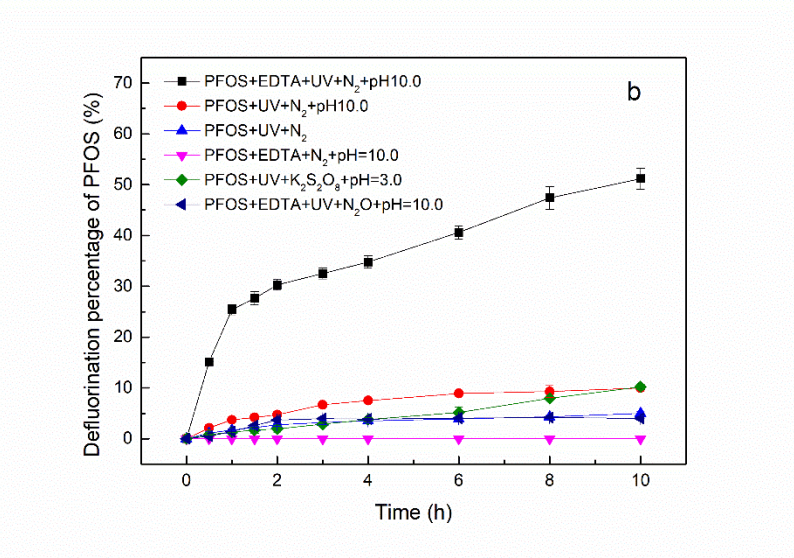


**Fig. 1** Irradiation-time dependence of decomposition (a) and defluorination percentages (b) of PFOS under different conditions. Error bars represent the standard deviations of triplicate assays.

Photo-reductive decomposition of PFOS at λ = 254 nm in the presence of EDTA was carried out under anoxic conditions. The experimental results obtained under these different conditions are shown in **Fig. 1**. The direct photolysis at λ = 254 nm for 10 h resulted in a relative decomposition percentage of PFOS of 15.97% and a defluorination percentage of 4.99%. These results are consistent with the weak absorption of 254 nm light by PFOS. Adjusting the solution pH to 10.0 results in the decomposition and defluorination percentages increasing to 20.97% and 9.99% after 10 h, respectively. In the absence of UV irradiation, no defluorination of PFOS was observed. However, UV irradiation at 254 nm in the presence of EDTA increased PFOS degradation to 78.08% after 10 h with a corresponding increase in defluorination to 51.19%. The rate of PFOS decomposition was relatively fast during the initial 0.5 h of irradiation. The

decomposition and defluorination percentages under UV/EDTA illumination after 0.5 h were 35.43% and 15.15%, respectively.

In order to determine the relative efficiency of UV/EDTA irradiation for PFOS degradation, we compared our approach to PFOS photolysis by UV/$K_2S_2O_8$. After 10 h of illumination at 254 nm, the decomposition and defluorination percentages via UV/$K_2S_2O_8$ photolysis were 49.3% and 10.2%, respectively. These results imply that the $e_{aq}^-$-mediated processes is effective in achieving defluorination compared to an oxidative process induced by persulfate photolysis (i.e., $SO^{\bullet}{}_4^-$ oxidation).

Similar experiment in the presence of nitrous oxide ($N_2O$) show that PFOS decomposition and defluorination were suppressed as shown in **Fig. 1** due to hydrated electrons scavenging by $N_2O$. Janata et al. [32] reported that $N_2O$ reacts with $e_{aq}^-$ with a second-order rate constant of $9.1\times10^9$ $M^{-1}s^{-1}$ (**Eq. 10**).

$$e_{aq}^- + N_2O \rightarrow OH^- + \cdot OH + N_2 \quad (k_2=9.1\times10^9\ M^{-1}s^{-1}) \qquad (10)$$

It is clear from these results that the $e_{aq}^-$ is the primary reducing agent that initiates the decomposition of PFOS.

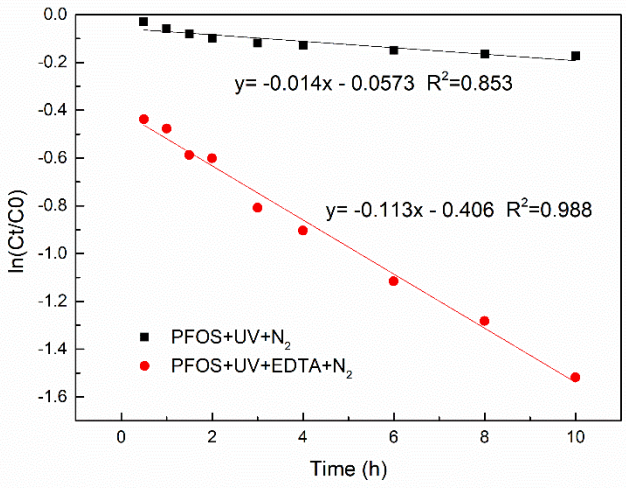

**Fig. 2** Kinetic modeling of PFOS degradation

The initial rate of decomposition of PFOS under optimal conditions follows simple pseudo first-order kinetics dependent on the [PFOS] as shown in **Fig. 2,** for which the hydrated electrons production is a zero-order process dependent on the photon flux intensity. The apparent reaction rate constant ($k_{obs}$) for PFOS decomposition was 0.113 $h^{-1}$, which corresponds to a half-life of 6.13 h. In comparison, $k_{obs}$ for the direct photolysis of PFOS was 0.014 $h^{-1}$ ($t_{1/2}$ = 49.29 h). The measured $k_{obs}$ values during UV/EDTA photolysis are compared to other photocatalytic processes in **Table 1**. Based on the comparison of **Table 1**, UV/EDTA photolysis showed clearly superior for the decomposition and defluorination of PFOS.

**Table 1. Comparison of photodecomposition of PFCs in this Study with other reported method**

| Method | Conditions | $k_{obs}$ ($h^{-1}$)[a] | Ref. |
|---|---|---|---|
| UV/EDTA | [PFOS]=10 μM, [EDTA] = 2.0 mM, λ=254 nm, 14W, pH=10, 25 ◦C | 0.113 | This study |
| Direct UV | [PFOS]=10 μM, λ = 254 nm, 14W, pH=7, 25 °C | 0.014 | This study |
| Direct UV | [PFOS]=2.5 μM, λ = 254 nm, 500W, pH=11.8, 100 ◦C | 0.91 | [17] |
| UV/$SO_3^{2-}$ | [PFOA]=38.7 μM, [$SO_3^{2-}$] = 10 mM, λ=200-400 nm, 250 W, pH=9.2, 25 ◦C | 0.045 | [33] |
| UV/Fe (III) | [PFOS]=20 μM, [$Fe^{3+}$] = 100 μM, λ=254 nm, 23 | 0.070 | [34] |

| | | | |
|---|---|---|---|
| | W, 25 ◦C | | |
| UV/alkaline 2-propanol | [PFOS]=40 μM, [alkaline 2-propanol]=90.7 mM , λ=254 nm, 32 W, 38-50 ◦C | 0.039 | [35] |
| UV/$K_2S_2O_8$ | [PFOS]=18.6 μM, [$K_2S_2O_8$] = 18.5 mM, λ=254 nm, 15 W×2, pH=3.1, 20 ◦C | 0.009 | [29] |
| UV/$NO_3^-$ | [PFOA]=5 ppm, [$NO_3^-$] = 100 mM, λ=254nm, 18 W, pH=6.3 | 0.025 | [36] |
| UV/SiC-graphene | [PFOA]=0.12 mM, catalyst dose = 0.5 g/L, λ=254nm, 5 W, pH=7 | 0.096 | [37] |
| UV/Pb-$BiFeO_3$/rGO | [PFOA]= 50 mg/L, catalyst dose = 0.1 g/L, rGO doping amount=5%, λ=254 nm, 5W, pH=4, 25 ◦C | 0.081 | [38] |
| VUV/sulfite | [PFOS]=37 μM, [$Na_2SO_3$] = 20 mM, λ=180 nm, 10 W, pH=10, 25 ◦C | 0.87 | [18] |

[a] Experimentally observed pseudo first-order rate constants.

The energy consumption required to decompose PFOS to half of its initial concentration is 84.18 kJ/μmol in UV/EDTA system, which is lower than those in many other photochemical technologies (**Table S1, Supplementary Material**). It indicated that UV/EDTA would be an economical process.

### 3.2 Products of EDTA degradation and toxicity assessment of UV/EDTA process

The UV/EDTA photolytic method appears to be relatively innocuous when used

for PFCs decomposition. Under UV irradiation, EDTA was depleted over time, and the decomposition followed the assumption of first-order kinetics with an apparent reaction rate constant of 1.700 $h^{-1}$. And the concentration of EDTA was below 2μM after 4 h. In addition, EDTA degraded with the formation of formaldehyde, ammonia and nitrate, which were detected during the treatment, as shown in **Fig. S2**. The concentration of formaldehyde was 3.93 mg/L at 10 h, which was lower than the third discharging level of 5 mg/L of National Standard of the People's Republic of China integrated wastewater discharge standard (GB 8978-1996) [39]. And the concentrations of ammonia and nitrate at 10 h were 6.21 mg/L and 2.87 mg/L, respectively.

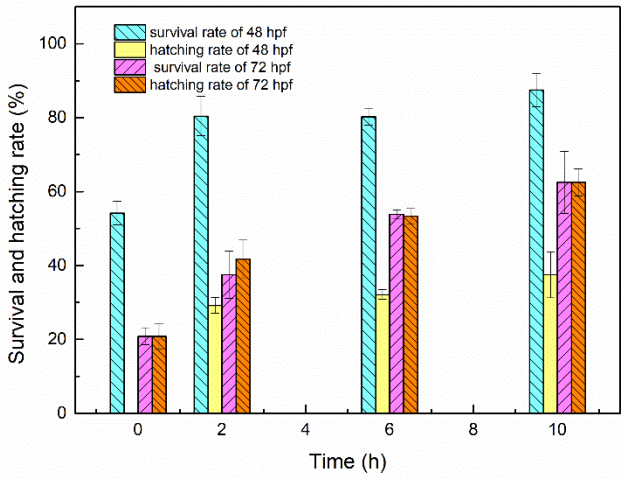


**Fig. 3.** The time-dependent toxicity of zebrafish embryos after 48 hpf and 72 hpf. Error bars represent standard deviations of triplicate assays.

To assess the toxicity of UV/EDTA process on zebrafish embryos were treated with series of samples for 72 hpf. As shown in **Fig. 3a**, UV/EDTA process exhibited increasing survival and hatching rates during treatment, the survival rates of zebrafish

embryos exposed to EDTA-PFOS solutions treated for 0 h, 2 h, 6 h, 8h were 20.83%, 37.5%, 54.16% and 62.50%, respectively. And the hatching rates of those were 20.83%, 41.67%, 53.28% and 62.50%, respectively. It was possibly due to the decomposition of PFOS. The difference of survival rate or hatching rate at 48 hpf and 72 hpf were mainly caused by the life characteristics of zebrafish embryos. Most of zebrafish embryos hatched after 72 hpf, while some hatched after 48 hpf. When they hatched, without the protection of membrane, they were easier exposed to products of EDTA-PFOS solution, leading to a significant difference of survival rates between 48 hpf and 72 hpf. In general, the increasing survival rates and hatching rates of zebrafish embryos exposed to series of EDTA-PFOS solution samples indicated that the toxic effect of this process was decreasing during treatment.

Thus, the UV/EDTA process can provide a relatively clean alternative process to achieve the photo-reductive degradation of PFOS.

### 3.3. Effects of primary reaction variables

#### 3.3.1 Effects of air

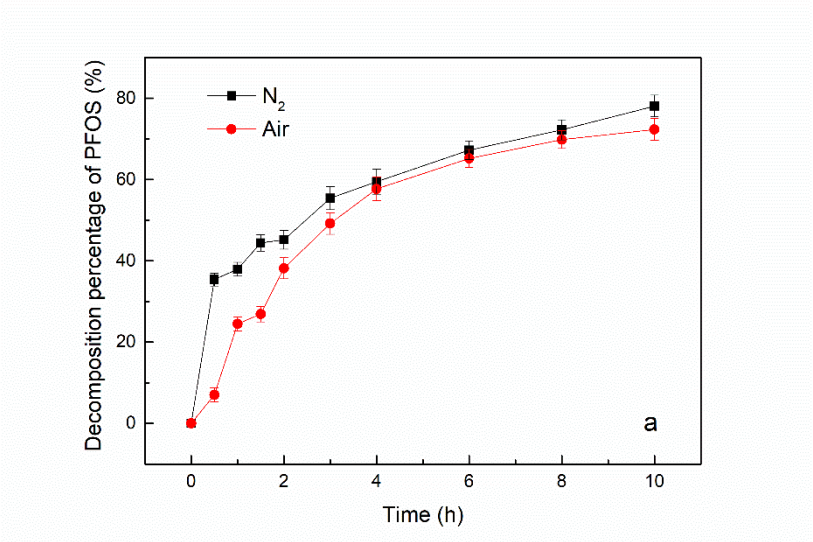

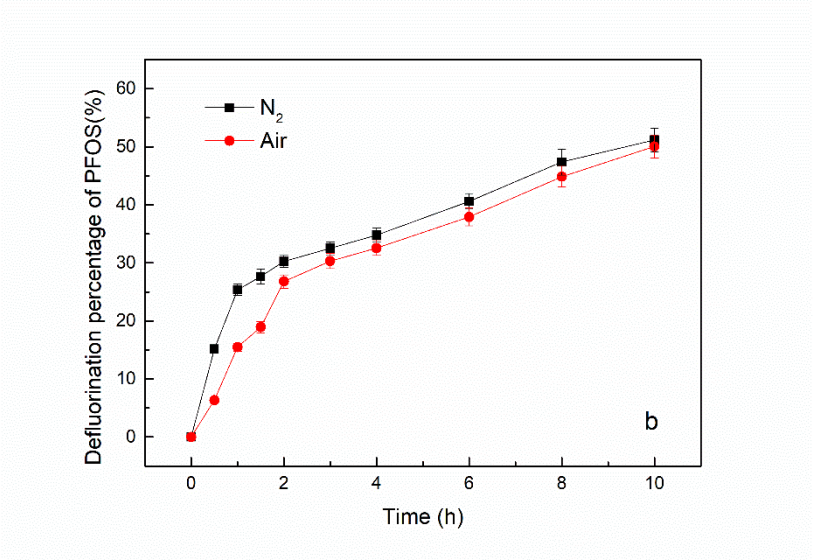


**Fig. 4.** Effects of air on the decomposition percentage (a) and defluorination percentages (b) of PFOS under the condition: PFOS (0.01 mM), EDTA (2.0 mM), UV irradiation, pH (10.0). Error bars represent standard deviations of triplicate assays.

Since hydrated electrons, $e_{aq}^-$, play a critical role in the decomposition of PFOS in the UV/EDTA process, $O_2$ can have a negative influence on the relative effectiveness of $e_{aq}^-$-mediated PFOS decomposition due to its impact as an $e_{aq}^-$ scavenger. To further explore the impact of oxygen on PFOS degradation was compared using an oxygen free $N_2$ purged system to a corresponding system in the presence of air. The reaction solution, in this care, was purged with $N_2$ for over the entire reaction. In comparison, the same reaction solution was not purged with $N_2$ and the reactor was opened to the laboratory atmosphere during the reaction. As shown in **Fig. 4**, the PFOS decomposition percentage after 10 h of irradiation in $N_2$ and air were 78.08% and 72.34%, respectively, while defluorination percentages of PFOS in $N_2$ and air were 51.19% and 50.06%, respectively. Clearly, there was little observed difference for

PFOS decomposition and defluorination under $N_2$ and air. These results indicate that there is no significantly negative impact of air on the degradation of PFOS during UV/EDTA photolysis. Our previous study has demonstrated that UV photolysis of NTA was efficient in PFOS decomposition, even in open air condition [27]. And this process exhibited better performance in PFOS defluorination in open air condition than UV/NTA process, with a defluorination percentage of 50.06%, while that of UV/NTA process was 35.85%. According to previous studies, the UV/iodide and UV/$SO_3^{2-}$ systems, which were shown to be efficient in decomposing PFOS, requires strict anoxic conditions. This result indicates that the application of UV/EDTA process for PFOS degradation could be practical because strict anoxic conditions are not required.

### 3.3.2 Effects of pH

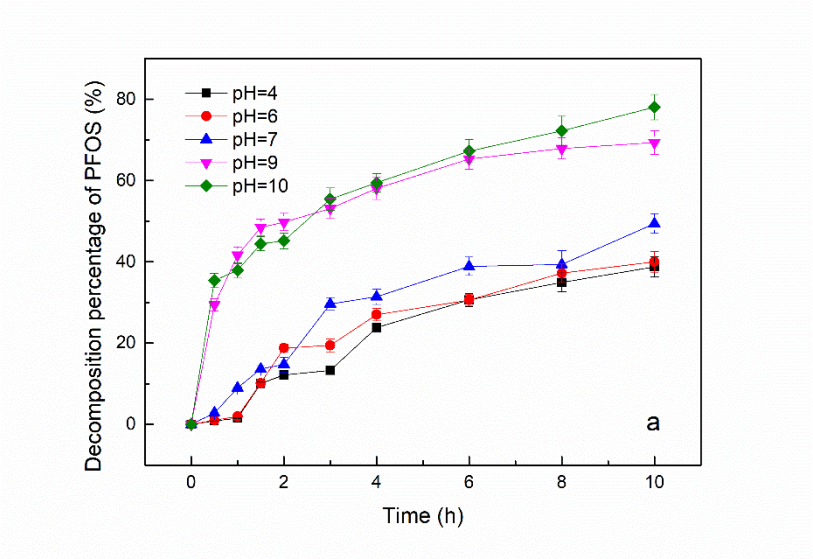

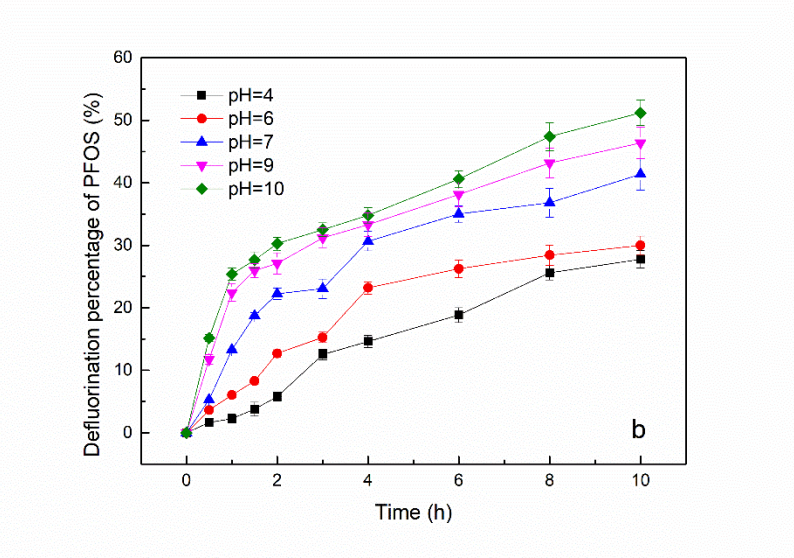


**Fig. 5.** Effects of initial pH on (a) PFOS decomposition versus time and (b) defluorination versus time under the following conditions: PFOS (0.01 mM), EDTA (2.0 mM), UV irradiation, $N_2$ purged. Error bars represent standard deviations of triplicate assays.

The effects the initial solution pH on PFOS decomposition and defluorination are shown in **Fig. 5**. These results show that the decomposition and defluorination of PFOS during UV/EDTA process is clearly pH-dependent. The decomposition percentages at pH of 9.0 and 10.0 were clearly much higher than those at pH of 4.0, 6.0 and 7.0. The decomposition percentage was highest under an initial pH of 10.0, while lowest observed rate was at an initial pH of 4.0. These results show that the $e_{aq}^-$-mediated decomposition of PFOS is more effective under alkaline conditions, which is a result that is consistent with previous report [17, 18]. The defluorination percentage after 10 h also increased with an increase in pH as follows for pH of 4, 6, 7, 9 and 10 after 10 h of irradiation were 27.77%, 29.99%, 41.38%, 46.38% and 51.19%, respectively.

The pH dependence of the percentage of PFOS decomposition can be explained in

terms of competitive reactions involving hydrated electron reactions. Under circum-neutral or acidic conditions, $e_{aq}^-$ can react with $H^+$ to form H· at a diffusion limited rate given the second-order rate constant for $e_{aq}^- + H^+ \rightarrow H\cdot$ of $k_3 = 2.3\times10^{10}\ M^{-1}s^{-1}$ (**Eq. 11**) [19]. Furthermore, hydrogen atom, H·, has a less negative reduction potential ($E(H^+/H\cdot) = -2.1$ V) [19] than that of $e_{aq}^-$ ($E(e_{aq}^-) = -2.9$ V). In addition, hydrogen atom has not been shown to be effective for decomposing PFOS, which was confirmed by the experiments carried out with $N_2O$ under acidic conditions (see details that are provided in the **Supplementary Material**). The kinetics of EDTA reacting with hydroxyl radical, ·OH, is also pH-dependent with a reported second-order reaction rate constant at pH 4 of $k_4 = 4\times10^8\ M^{-1}s^{-1}$, $k_5 = 2\times10^9\ M^{-1}s^{-1}$ at pH=9, and $k_6 = 5.7\times10^9\ M^{-1}s^{-1}$ at pH=11 [40, 41]. A faster hydroxyl radical rate at high pH is consistent with our current observations. In conclusion, under circum-neutral or acidic conditions, $e_{aq}^-$ would be quenched by lots of $H^+$. And under alkaline condition, EDTA, which serves primarily as a hydroxyl radical scavenger and inhibits the recombination of $e_{aq}^-$ with hydroxyl radical resulting in an increased average photolytic lifetime for $e_{aq}^-$, has a faster reaction rate with hydroxyl radical at high pH.

A change in pH was measured during the photolysis of the EDTA-PFOS solution that was set at initial pH values of 4 and 6 as shown in **Fig. S4**. The pH of the solution of EDTA-PFOS increased rapidly and stabilized around 8 during treatment. The changes of pH are probably attributed to formation of basic products such as amides [42] and to the reaction of $e_{aq}^-$ with $H^+$ leading to an increase in pH (**Eq. 11)**. Again, the pH rose from pH 4 and 6 to pH in the first 2 h of photolysis. This interpretation is in

good agreement with the observed results in that PFOS decomposition and defluorination percentages were low during the first 2 h and then increased after that.

The UV/EDTA process is clearly quite effective in inducing PFOS decomposition and defluorination over a wide range of pH when compared to other photo-reductive processes, such as the UV/$SO_3^{2-}$ and UV/NTA system. For a direct comparison, the UV/EDTA system obtained PFOS decomposition percentages at pH 4, 6 and 7 after 10 h of irradiation of 38.80%, 40.03%, and 49.45%, respectively. While in UV/NTA process, PFOS decomposition percentages at pH 7 was below 10% [27]. In the case of the UV/$SO_3^{2-}$ system, PFOS decomposition and defluorination was reported to be negligible at pH 7 [43].

Since UV/EDTA photolysis of PFOS degradation can be carried out over a wide pH range in the presence of air it may provide a practical solution for the elimination of PFOS from contaminated water sources.

### 3.4. Mechanism of PFOS degradation in UV/EDTA system

#### 3.4.1 Laser flash photolysis

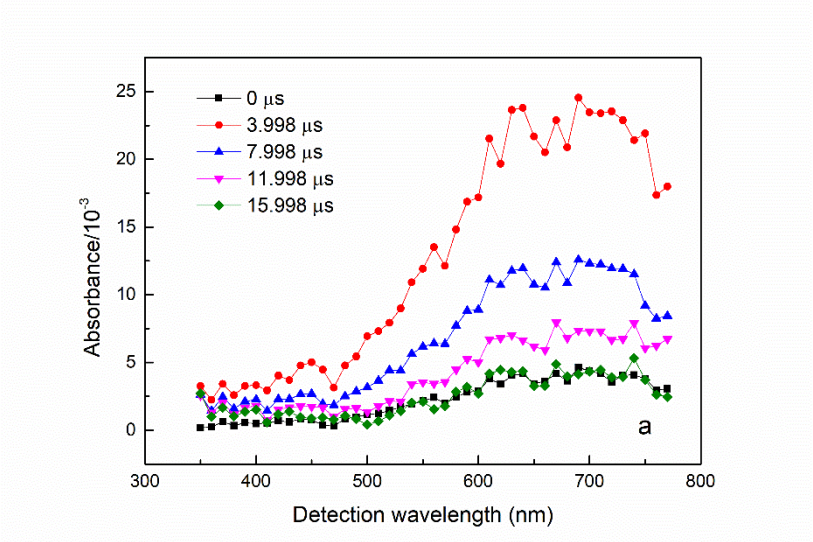

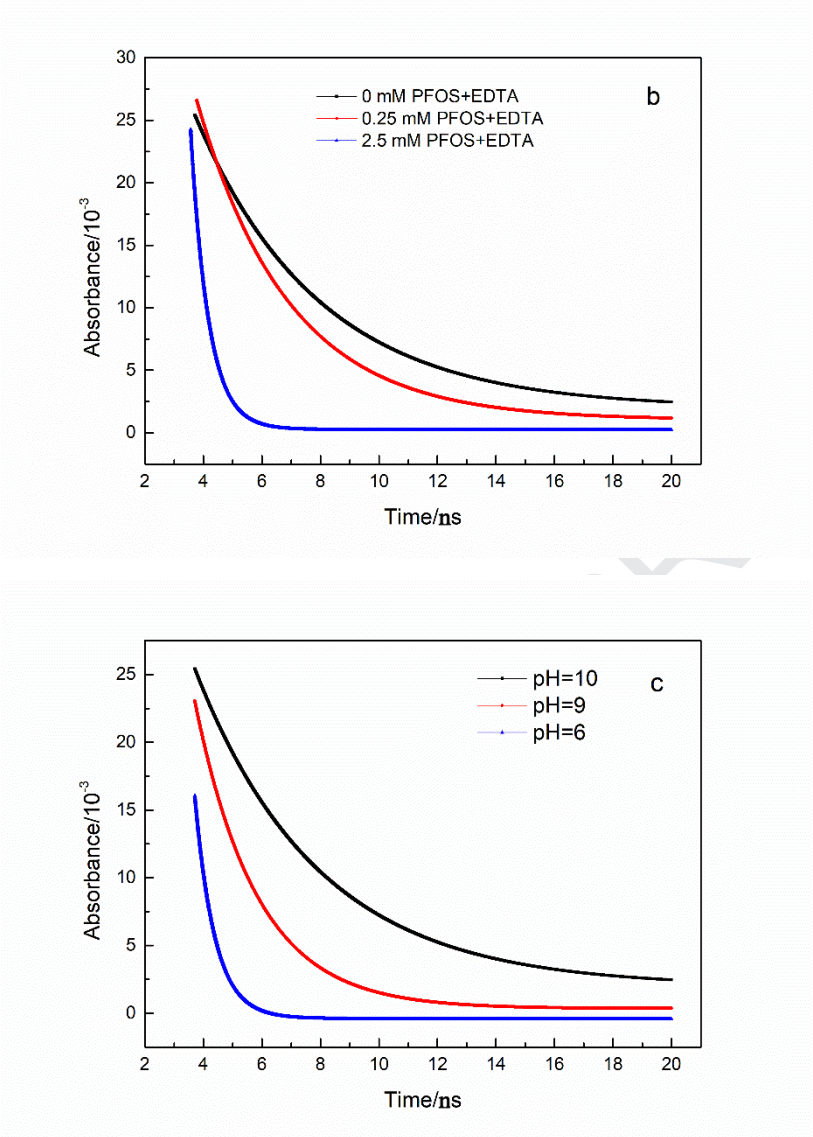


**Fig. 6.** (a) Transient absorption spectra following the laser flash photolysis of 50 mM EDTA solution at pH 10.0. (b) The decays of $e_{aq}^-$ detected at 690 nm in the presence of PFOS with different concentrations. (c) The decays of $e_{aq}^-$ detected at 690 nm at different pH conditions. The transient absorption curves are fitted.

As shown in **Fig. 6a**, the wide absorption band with a peak at around 690 nm is assigned to the $e_{aq}^-$, which is consistent with theoretical and experimental $e_{aq}^-$ absorption spectra [44, 45]. The absorption peak of $e_{aq}^-$ was not observed in pure water

or a buffered solution due to the rapid recombination of $e_{aq}^-$ with ·OH, H· and $H_3O^+$ (**Eq. 4-6**). The time-dependent transient decay of $e_{aq}^-$ was followed at 690 nm as a function of the [PFOS] (**Fig. 6b**). The decay rate of $e_{aq}^-$ increased with increasing [PFOS]. These results clearly establish the role of of $e_{aq}^-$ in the decomposition of PFOS.

The concentration of $e_{aq}^-$ as detected 690 nm decreases due to the recombination of $e_{aq}^-$ with ·OH, H·, and $H_3O^+$ (**Eq. 4-6**). In the UV/EDTA photolytic process, EDTA scavenges ·OH given the magnitude of the second-order rate constant for reaction ($k_7 = 3.3\times10^9\ M^{-1}s^{-1}$ at pH=8) [41]. Thus, the scavenging of EDTA towards ·OH can protect $e_{aq}^-$ from being quenched by ·OH. Thus, EDTA has the net effect of increasing the transient lifetime $e_{aq}^-$ during UV/EDTA photolysis (**Fig. 6**). For instance, the half-life of $e_{aq}^-$ during UV/EDTA is close to 4.2 μs, while during UV/KI process the reported lifetime is less than 2 μs [46]. Therefore, it is clear that EDTA prolongs the survival time of $e_{aq}^-$ by scavenging ·OH resulting in an increased steady-state concentration of $[e_{aq}^-]_{ss}$. This explains the apparently low transient quantum yield of $e_{aq}^-$ during UV/EDTA photolysis. However, the net effect is an efficient method for PFOS degradation.

Additional transient measurements show that the initial absorbance and lifetime of the $e_{aq}^-$ at 690 nm increased with an increasing solution pH (**Fig. 6c**). These results show the scavenging of $e_{aq}^-$ in increases as a function the proton activity (i.e., with decreasing pH). The transient kinetic results also confirm that the photolytic degradation of PFOS mediated by $e_{aq}^-$ increases under basic conditions.

### 3.4.2 Decomposition mechanism

Hydrated electrons, $e_{aq}^-$ generated by direct photolysis rapidly recombine with other primary species including ·OH, H· and $H_3O^+$. However, the reaction of $e_{aq}^-$ with ·OH accounts for over 82% ± 3% of the loss of $e_{aq}^-$ [47]. Previous studies have demonstrated that EDTA can serve as an electron donor in photocatalytic reactions [48-51]. Furthermore, EDTA reacts readily with ·OH [52]. For example, the rate constant for the reaction of ·OH and tert-butanol is $5\times10^8$ $M^{-1}s^{-1}$ [53]. This constant is roughly an order of magnitude lower than that of ·OH with EDTA ($5.7\times10^9$ $M^{-1}s^{-1}$) [41]. Thus, EDTA is clearly a more efficient quencher of ·OH.

**Fig. S5** shows a comparison of the PFOS decomposition percentage with the corresponding rate of PFOS defluorination. The PFOS decomposition percentage is higher as a function of time. This result shows that even though PFOS was degraded, it was not completely defluorinated. It is obvious that other perfluorinated containing intermediates are generated at the same time that $F^-$ is produced during the photolytic degradation of PFOS. Short-chain-length perfluorinated intermediates such as PFOA ($C_7F_{15}COO^-$), PFHxS ($C_6F_{13}SO_3^-$), PFHpA ($C_6F_{13}COO^-$) and PFHxA ($C_5F_{11}COO^-$) were detected in UV/EDTA process (**Fig. S6b**). In direct photolysis process, in addition to these, PFBA ($C_3F_7COO^-$) and PFPrA ($C_2F_5COO^-$) were also detected, as shown in **Fig. S6a**. Compared to the direct photolysis of PFOS in the absence of EDTA, the concentrations of the F-containing intermediates during UV/EDTA photolysis were found to be much lower. These results show that EDTA enhances the degradation of the F-containing intermediates produced during the decomposition of PFOS. Moreover, as shown in **Fig. S6b**, the formed short-chain perfluorinated compounds increased at

first and then decreased over time. The peak of individual species appearing earlier with longer chain illustrated that PFOS decomposed stepwise over the reaction time. However, in direct photolysis of PFOS, as shown in **Fig. S6a**, these shorter-chain compounds did not diminish over time. It was possibly due to that PFOA and PFHxA with longer-chain were easier to be decomposed, while PFBA and PFPrA with shorter-chain were harder to be decomposed, leading to the accumulation of shorter-chain perfluorinated compounds. Based on the concentrations of PFOS, F-containing intermediates and $F^-$, the mass balance of F was calculated by **Eq. 9**, as shown in **Fig. S7**. The loss of F recovery during the reaction are probably attributed to the formation of partially fluorinated intermediates (C1 to C5). In view of the distribution of intermediates and the fluorine mass balance, PFOS and its intermediates are most likely decomposed in a stepwise manner.

The reaction of $e_{aq}^-$ with PFOS may result in defluorination, desulfonation, or C-C bond scission [43, 54]. The PFOS anion has been previously shown to react with $e_{aq}^-$ leading to the formation of $C_8F_{17}SO^{\bullet 2-}_3$, which, in turn, undergoes further dissociation into $C_8F_{17}^-$ and $SO^{\bullet -}_3$ [16, 43, 55] . These two fragments have a lower $\Delta E$ = -30.99 kcal/mol [42] compared to alternative fragmentation products. This outcome is most likely due to the lower bond energy of C-S (272 kJ/mol) compared with that of C-C (346 kJ/mol) and C-F (532 kJ/mol) bonds. As a consequence, $C_8F_{17}^-$ dissociates and then forms PFOA via the hydrolysis reactions (**Eq. 12-16**) [43]. In the case of PFOA, the carbon atoms are saturated and therefore unable to provide vacant orbitals to accommodate an extra electron. However, a fluorine atom of a fluoro-

methylene moiety is capable for reacting with an electron because of its high electron affinity [56]. The net result is that fluorine atoms, instead of carbon atoms, become the dynamic reaction centers. Furthermore, the inductive effect of carbonyl group of the carboxylate of PFOA that withdraws electron density from the $\alpha$-position C-F bond making that site more susceptible to attack by $e_{aq}^-$. This leads to the dissociation of a fluorine from the α-$CF_2$- forming fluoride leading to the formation of $C_7F_{13}H_2COOH$ (**Eq. 17-20**) [20, 43]. $C_7F_{13}H_2COOH$ can be excited to form free radicals, such as $\cdot C_6F_{13}$, methylene radical ($CH_2$) and ·COOH under UV irradiation (**Eq. 22**) [43]. The recombination of $\cdot C_6F_{13}$ and $SO_3^{\bullet -}$ is likely responsible for the formation of $C_6F_{13}SO_3^-$ (PFHxS) (**Eq. 22**) [43], which was experimentally detected. Subsequently, the concentration of PFHxS rose above that of PFOA. In addition, the fluoro-methylene radicals, $\cdot CH_2\cdot$ are reactive species leading to the formation of methyl radicals ($\cdot CH_3$), which then react with formyl radical, ·COOH, to form $CH_3COOH$ (**Eq. 23-24**) [43]. The various intermediates are eventually mineralized to formate, acetate, fluoride, and sulfate after the longer time reaction times as shown in **Fig. S8**.

$$C_8F_{17}SO_3^- + e_{aq}^- \rightarrow C_8F_{17}SO_3^{\bullet 2-} \quad (12)$$

$$C_8F_{17}SO_3^{\bullet 2-} \rightarrow C_8F_{17}^- + SO_3^{\bullet -} \quad (13)$$

$$C_8F_{17}^- + H_3O^+ \rightarrow C_8F_{17}OH + 2H\bullet \quad (14)$$

$$C_8F_{17}OH \rightarrow C_7F_{15}COF + HF \quad (15)$$

$$C_7F_{15}COF + H_2O \rightarrow C_7F_{15}COOH + HF \quad (16)$$

$$C_7F_{15}COOH + e_{aq}^- \rightarrow \bullet C_7F_{14}COOH + F^- \quad (17)$$

$$\bullet C_7F_{14}COOH + H_2O \rightarrow \bullet C_7F_{14}HCOOH + \bullet OH \quad (18)$$

$$C_7F_{14}HCOOH + e_{aq}^- \rightarrow \bullet C_7F_{13}HCOOH + F^- \quad (19)$$

$$\bullet C_7F_{13}HCOOH + H_2O \rightarrow C_7F_{13}H_2COOH + \bullet OH \quad (20)$$

$$C_7F_{13}H_2COOH \rightarrow \bullet C_6F_{13} + \bullet CH_2 \bullet + \bullet COOH \quad (21)$$

$$\bullet C_6F_{13} + SO_3^{\bullet -} \rightarrow C_6F_{13}SO_3^- \quad (22)$$

$$\bullet CH_2 \bullet + H \bullet \rightarrow \bullet CH_3 \quad (23)$$

$$\bullet CH_3 + \bullet COOH \rightarrow CH_3COOH \quad (24)$$

### 3.5 Structure-activity relationship

In order to further investigate the mechanism of PFOS degradation during UV/EDTA photolysis, the photodecomposition of other perfluorochemicals and the degradation of PFOS with UV/tetramethylethylenediamine (TMEDA) and UV/hydroxyethyl ethylenediamine triacetic acid (HEDTA) were also studied.

#### 3.5.1 Degradation of PFOS, PFHxS and PFBS

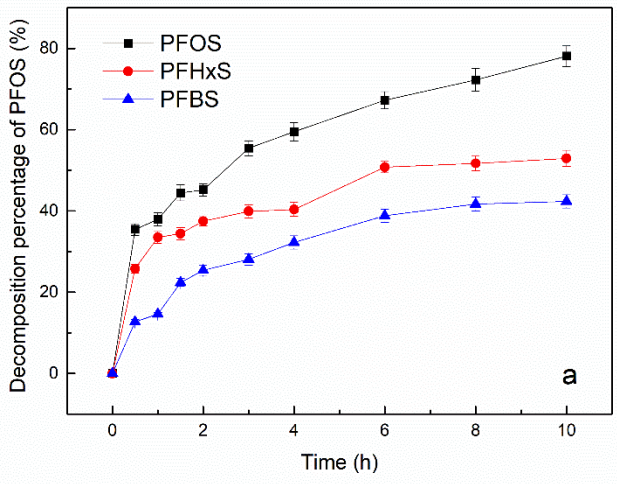

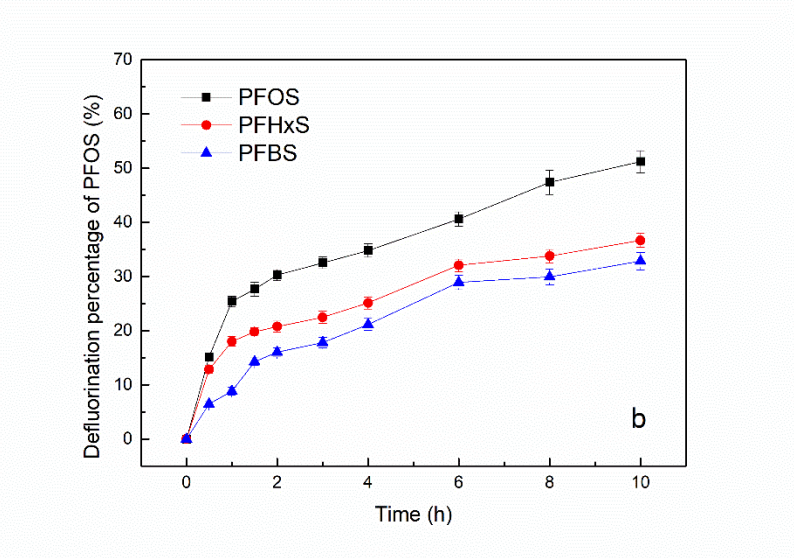


**Fig. 7.** Irradiation-time dependence of decomposition (a) and defluorination percentage (b) of PFOS, PFHxS and PFBS under the condition: PFOS/PFHxS/PFBS (0.01 mM), EDTA (2.0 mM), UV irradiation, $N_2$ purged, pH (10.0). Error bars represent standard deviations of triplicate assays.

The decomposition of other perfluoroalkyl sulfonates, PFHxS ($C_6F_{11}SO_3^-$) and PFBS ($C_4F_9SO_3^-$), was also investigated. As illustrated in **Fig. 7**, decomposition percentage and defluorination percentage of PFOS, PFHxS, PFBS during UV/EDTA photolysis were compared. The decomposition percentage and defluorination percentage of PFOS, PFHxS and PFBS showed a strong dependence on chain length, while the decomposition kinetics of perfluoroalkyl sulfonates increased with increasing chain length ($k_{app}^{PFBS}$ = 0.0506 $h^{-1}$, $k_{app}^{PFHxS}$ = 0.0583 $h^{-1}$, $k_{app}^{PFOS}$ = 0.1275 $h^{-1}$). This trend is consistent with that reported in a previous study by Park et al. [13]. Bentel et al. [6] reported that perfluoroalkyl sulfonates with longer chain, lower bond dissociation energies (BDEs) for both primary (i.e., bonds on the terminal -$CF_3$) and

secondary (i.e., bonds on -$CF_2$-) C-F bonds were observed. Paul et al. [57] reported that the central -$CF_2$- linkage in a fluoroalkyl chain had the highest electron affinity. In addition, the removal of PFBS and PFHxS appeared to essentially stop after 6 hours. It may be attributed to the degradation of EDTA. EDTA degraded with the formation of IDA and glycine [58]. IDA and glycine were proved that they could accelerate the photo-reductive PFOS decomposition [27], but they were much less efficient than EDTA. Due to perfluoroalkyl sulfonates with shorter chain had higher BDEs for both primary and secondary C-F bonds, IDA and glycine were probably ineffective in promoting PFBS and PFHxS decomposition. Thus, the decomposition of PFBS and PFHxS slowed down and appeared to stop after 6 h with EDTA consumed, while PFOS with longer chain was still slightly decomposed. Therefore, these trends may explain why the decomposition and defluorination rates were found to be faster for longer chain perfluoroalkyl sulfonates.

### 3.5.2 UV/EDTA, UV/HEDTA, and UV/TMEDA photolysis

The photolytic degradation of PFOS in the presence of tetramethylethylenediamine (TMEDA) and N-(2-Hydroxyethyl) ethylenediaminetriacetic acid (HEDTA) were also studied. TMEDA and HEDTA are similar with EDTA in terms of molecular structure. The primary differences are that the hydrogen atoms connected to the nitrogen in ethylenediamine are replaced by other functional groups. The structural configurations of TMEDA, HEDTA and EDTA are given in **Table S2**.

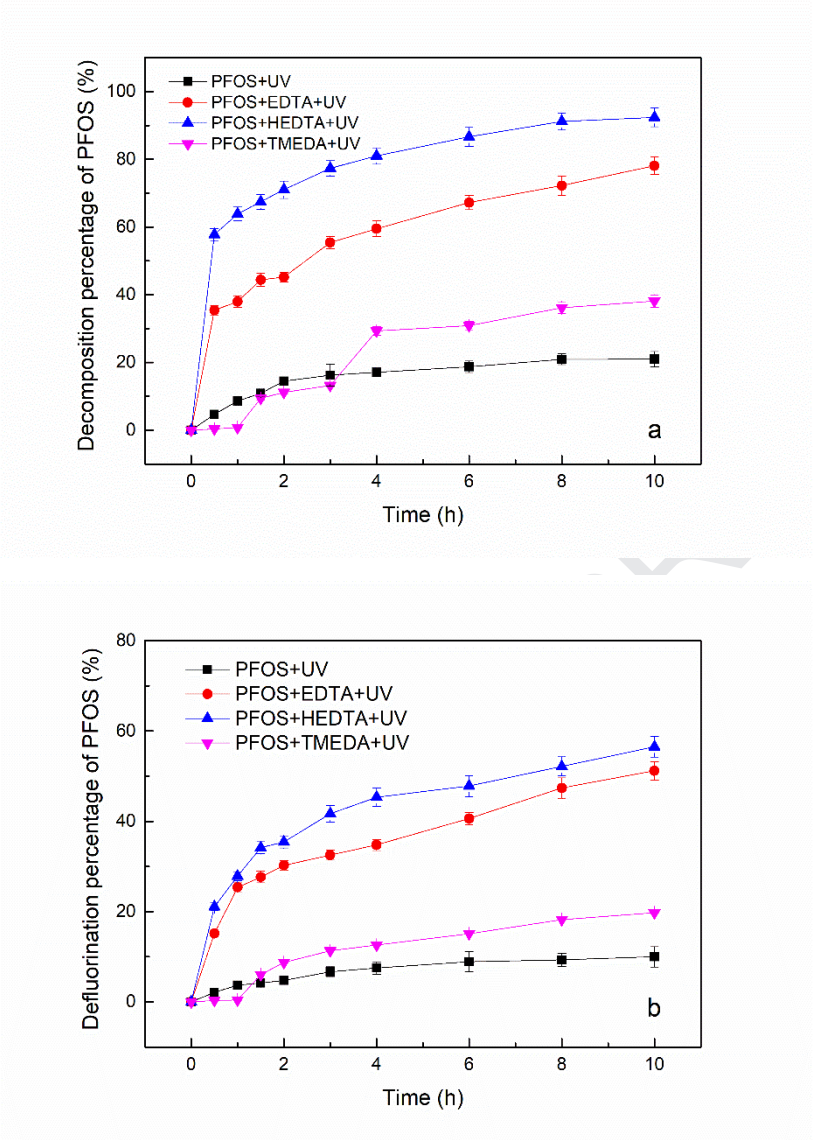


**Fig. 8.** Decomposition percentage (a) and defluorination percentage (b) of PFOS in UV, UV/EDTA, UV/HEDTA and UV/TMEDA systems. Conditions: EDTA, HEDTA and TMEDA (2.0 mM), PFOS (0.01 mM), UV irradiation, $N_2$ prebubbled, pH (10.0). Error bars represent standard deviations of triplicate assays.

**Fig. 8** compares the photolytic decomposition percentage (a) and defluorination percentage (b) of PFOS by UV alone (a control experiment), UV/EDTA, UV/HEDTA, and UV/TMEDA during photolysis as a function to time. The presence of EDTA clearly

leads to an accelerated decomposition and defluorination compared with the control experiment. In comparison, UV/TMEDA photolysis produced a slight increase in PFOS decomposition and defluorination. For comparison, after 10 h of photolysis, the PFOS degradation and defluorination percentages in the presence of EDTA were 78.1% and 51.2%, respectively, whereas TMEDA photolysis resulted in corresponding percentages of 38.1% and 19.8%, respectively. This overall result may be attributed to the role of methylene groups ($CH_2$) attached nitrogen atoms in EDTA is connected to one more carboxyl group than in the case of TMEDA. Therefore, the carboxyl group attached to the α-C of amine determines the efficiency in promoting PFOS photodegradation. The methylene group can also provide a reactive site for attack by ·OH leading to H-atom abstraction [59]. Whereas, the methyl ($-CH_3$) group in TMEDA provides a less susceptible site for ·OH radical attack and subsequent H-atom abstraction. In spite of the less favorable reaction sites, TMEDA still showed a slight enhancement of PFOS decomposition and defluorination over time. This could be attributed to the lone pair on the nitrogen atom that should provide a susceptible site for an electrophilic attack by ·OH [11].

HEDTA, in contrast is slightly more effective in promoting the photolytic decomposition of PFOS than EDTA as shown in **Fig. 8**. The 10-h PFOS decomposition percentages in the presence of EDTA and HEDTA were 78.1% and 92.4%, respectively, while the corresponding 10-h defluorination percentages were 51.2% and 56.5%, respectively. HEDTA has a similar chemical structure with that of EDTA. The only difference between EDTA and HEDTA is a carbonyl group (C=O) to a methylene

group. The carbonyl group inductively withdraws electron density from the neighboring N, which effectively reducing the reactivity of EDTA with ·OH. In contrast, the additional methylene group in -$CH_2CH_2OH$ linkage offers a more reactive site for ·OH attack, thus increasing the reactivity of HEDTA with ·OH. In support of this argument we note that the rate constant for the reaction of ·OH and HEDTA ($k_8$ = $8.2\times10^9$ $M^{-1}s^{-1}$, pH=11) is slightly higher than that of ·OH reacting with EDTA ($k_6$ = $5.7\times10^9$ $M^{-1}s^{-1}$, pH=11) [41]. The amines and the methylenes play a crucial role in promoting PFOS photodegradation, which allow for an effective attack by ·OH via H-atom abstraction from an amine or from a methylene.

**4. Conclusions**

This study demonstrates that the photolytic decomposition of PFOS during UV photolysis at 254 nm in the presence of EDTA is enhanced compared to alternative photolytic methods. UV/EDTA photolysis degraded 78.1% of PFOS with a defluorination percentage of 51.19% after 10 h of low intensity irradiation. The use of EDTA to enhance the photodecomposition of PFOS could have practical engineering applications since PFOS decomposition is only slightly reduced under oxidic conditions. In addition, UV photolysis of PFOS in the presence of EDTA leads to a higher fraction of PFOS that is decomposed and defluorinated over a wide range of pH compared to alternative photo-reductive processes that depend on iodide or sulfite photolysis. EDTA increases the transient lifetime of the photo-generated hydrated electrons due to its role as an ·OH radical scavenger.

**Acknowledgements**

The authors gratefully acknowledge Prof. Weiming Zhang and Dr. Bingdang Wu from State Key Laboratory of Pollution Control and Resource Reuse, School of the Environment, Nanjing University, Nanjing 210023, China, for their kind assistance on the LFP result analysis. This study was supported by the National Natural Science Foundation of China (Project No. 21677109), the Fundamental Research Funds for the Central Universities (Project No. 22120180118, No. 22120180247) and the Major Science and Technology Program for Water Pollution Control and Treatment (Project No. 2018ZX 07109-001-03).

## References

[1] B.D. Key, R.D. Howell, C.S. Criddle, Fluorinated organics in the biosphere, Environ. Sci. Technol. 31 (1997) 2445-2454.

[2] C.A. Moody, J.A. Field, Perfluorinated surfactants and the environmental implications of their use in fire-fighting foams, Environ. Sci. Technol. 34 (2000) 3864-3870.

[3] J.P. Giesy, K. Kannan, Perfluorochemical surfactants in the environment, Environ. Sci. Technol., 36 (2002) 146-152.

[4] S. Fujii, C. Polprasert, S. Tanaka, N.P.H. Lien, Y. Qiu, New POPs in the water environment: Distribution, bioaccumulation and treatment of perfluorinated compounds-A review paper, J. Water Supply Res. Technol. 56 (2007) 313-326.

[5] P. Wardman, Reduction potentials of one-electron couples involving free radicals in aqueous solution, J. Phys. Chem. Ref. Data 18 (1989) 1637-1755.

[6] M.J. Bentel, Y.C. Yu, L.H. Xu, Z. Li, B.M. Wong, Y.J. Men, J.Y. Liu, Defluorination of per- and polyfluoroalkyl substances (PFASs) with hydrated electrons: Structural dependence and implications to PFAS remediation and management, Environ. Sci. Technol. 53 (2019) 3718-3728.

[7] C. Lau, K. Anitole, C. Hodes, D. Lai, A. Pfahles-Hutchens, J. Seed, Perfluoroalkyl acids: A review of monitoring and toxicological findings, Toxicol. Sci. 99 (2007) 366-394.

[8] M.E. Andersen, J.L. Butenhoff, S.C. Chang, D.G. Farrar, G.L. Kennedy, C. Lau, G.W. Olsen, J. Seed, K.B. Wallace, Perfluoroalkyl acids and related chemistries-toxicokinetics and modes of action, Toxicol. Sci. 102 (2008) 3-14.

[9] United Nations Environment Programme, The Environment in the News, from http://www.unep.org/cpi/briefs/ 11 May 2009.

[10] S.H. Ma, M.H. Wu, L. Tang, R. Sun, C. Zang, J.J. Xiang, X.X. Yang, X. Li, G. Xu, EB degradation of perfluorooctanoic acid and perfluorooctane sulfonate in aqueous solution, Nucl. Sci. Technol. 28 (2017) 137.

[11] M. Trojanowicz, I. Bartosiewicz, A. Bojanowska-Czajka, K. Kulisa, T. Szreder, K. Bobrowski, H. Nichipor, H. Nichipor, G. Nalecz-Jawecki, S. Meczynska-Wielgosz, J. Kisala, Application of ionizing radiation in decomposition of perfluorooctanoate (PFOA) in waters, Chem. Eng. J. 357 (2019) 698-714.

[12] Z. Song, H.Q. Tang, N. Wang, L.H. Zhu, Reductive defluorination of perfluorooctanoic acid by hydrated electrons in a sulfite-mediated UV photochemical system, J. Hazard. Master. 262 (2013) 332-338.

[13] H. Park, C.D. Vecitis, J. Cheng, W.Y. Choi, B.T. Mader, M.R. Hoffmann, Reductive defluorination of aqueous perfluorinated alkyl surfactants: Effects of ionic headgroup and chain length, J. Phys. Chem. A 113 (2009) 690-696.

[14] H.T. Tian, C. Gu, Effects of different factors on photodefluorination of perfluorinated compounds by hydrated electrons in organo-montmorillonite system, Chemosphere 191 (2018) 280-287.

[15] H.T. Tian, J. Gao, H. Li, S.A. Boyd, C. Gu, Complete defluorination of perfluorinated compounds by hydrated electrons generated from 3-Indole-acetic-acid in organomodified montmorillonite, Sci. Rep. 6 (2016) 32949.

[16] B. Han, J.K. Kim, Y. Kim, J.S. Choi, K.Y. Jeong, Operation of industrial-scale electron beam wastewater treatment plant, Radiat. Phys. Chem. 81 (2012) 1475-1478.

[17] X.J. Lyu, W.W. Li, P.K. Lam, H.Q. Yu, Insights into perfluorooctane sulfonate

photodegradation in a catalyst-free aqueous solution, Sci. Rep. 5 (2015) 9353.

[18] Y.R. Gu, T.Z. Liu, H.J. Wang, H.L. Han, W.Y. Dong, Hydrated electron based decomposition of perfluorooctane sulfonate (PFOS) in the VUV/sulfite system, Sci. Total Environ. 607-608 (2017) 541-548.

[19] G.V. Buxton, C.L. Greenstock, W.P. Helman, A.B. Ross, Critical review of rate constants for reactions of hydrated electrons, hydrogen atoms and hydroxyl radicals (•OH/•$O^-$ in aqueous solution), J. Phys. Chem. Ref. Data 17 (1988) 513-886.

[20] Y. Qu, C.J. Zhang, F. Li, J. Chen, Q. Zhou, Photo-reductive defluorination of perfluorooctanoic acid in water, Water Res. 44 (2010) 2939-2947.

[21] X.J. Lyu, W.W. Li, P.K.S. Lam, Photodegradation of perfluorooctane sulfonate in environmental matrices, Sep. Purif. Technol. 151 (2015) 172-176.

[22] J.G. Hollowell, N.W. Staehling, W.H. Hannon, W.H. Flanders, E.W. Gunter, G.F. Maberly, L.E. Braverman, S. Pino, D.T. Miller, P.L. Garbe, D.M. DeLozier, R.J. Jackson, Iodine nutrition in the United States. Trends and public health implications: Iodine excretion data from national health and nutrition examination surveys I and III (1971–1974 and 1988–1994), J Clin Endocrinol Metab. 83 (1998) 3401-3408.

[23] H. Burgi, T. Schaffner, J.P. Seiler, The toxicology of iodate: A review of the literature, Thyroid 11 (2001) 449-456.

[24] A.F. Gunnison, Sulfite toxicity - A critical review of invitro and invivo date, Food Cosmet. Toxicol. 19 (1981) 667-682.

[25] F. Gobert, S. Pommeret, G. Vigneron, S. Buguet, R. Haidar, J.C. Mialocq, I. Lampre, M. Mostafaviet, Nanosecond kinetics of hydrated electrons upon water photolysis by high intensity

femtosecond UV pulses, Res. Chem. Intermed. 27 (2001) 901-910.

[26] G.V. Buxton, M. Spotheim-Maurizot, M. Mostafavi, T. Douki, J. Belloni (Eds.), An overview of the radiation chemistry of liquids, Radiation Chemistry: From Basics to Applications in Material and Life Sciences, EDP Sciences (2008).

[27] Z.Y. Sun, C.J. Zhang, L. Xing, Q. Zhou, W.B. Dong, M.R. Hoffmann, UV/nitrilotriacetic acid process as a novel strategy for efficient photoreductive degradation of perfluorooctanesulfonate, Environ. Sci. Technol. 52 (2018) 2953-2962.

[28] B. Behmand, P. Cloutier, S. Girouard, Hydrated electrons react with high specificity with cisplatin bound to single-stranded DNA, J. Phys. Chem. 117 (2013) 15994-15999.

[29] S.W. Yang, J.H. Cheng, J. Sun, Y.Y. Hu, X.Y. Liang, Defluorination of aqueous perfluorooctanesulfonate by activated persulfate oxidation, Plos One 8 (2013) 10.

[30] L. Wang, C.L. Zhou, H.Q. Chen, J.G. Chen, J. Fu, B. Ling, Determination of formaldehyde in aqueous solutions by a novel fluorescence energy transfer system, Analyst 135 (2010) 2139-2143.

[31] HJ 535-2009, National environmental protection standards of the People's Republic of China, 2009.

[32] E. Janata, R.H. Schuler, Rate constant for scavenging $e_{aq}^-$ in $N_2O$-saturated solutions, J. Phys. Chem. 86 (1982) 2078-2084.

[33] Y.R. Gu, T.Z. Liu, Q. Zhang, W.Y. Dong, Efficient decomposition of perfluorooctanoic acid by a high photon flux UV/sulfite process: Kinetics and associated toxicity, Chem. Eng. J. 326 (2017) 1125-1133.

[34] L. Jin, P.Y. Zhang, T. Shao, S.L. Zhao, Ferric ion mediated photodecomposition of aqueous perfluorooctane sulfonate (PFOS) under UV irradiation and its mechanism, J. Hazard. Master. 271

(2014) 9-15.

[35] T. Yamamoto, Y. Noma, S.-Y. Sakai, Y. Shibata. Photodegradation of perfluorooctane sulfonate by UV irradiation in water and alkaline 2-propanol, Environ. Sci. Technol. 41 (2007) 5660-5665.

[36] A.M. Li, Z. Zhang, P.F. Li, L.J. Cai, L.Z. Zhang, J.M. Gong, Nitrogen dioxide radicals mediated mineralization of perfluorooctanoic acid in aqueous nitrate solution with UV irradiation, Chemosphere 188 (2017) 367-374.

[37] D. Huang, L. Yin, J. Niu, Photoinduced hydro defluorination mechanisms of perfluorooctanoic acid by the SiC/Graphene catalyst, Environ. Sci. Technol. 50 (2016) 5857-5863.

[38] E.X. Shang, Y. Li, J.F. Niu, S. Li, G.S. Zhang, Photocatalytic degradation of perfluorooctanoic acid over Pb-$BiFeO_3$/rGO catalyst: kinetics and mechanism, Chemosphere 211 (2018) 34-43.

[39] GB 8978-1996, Integrated wastewater discharge standard, National Standard of the People's Republic of China, 1996.

[40] P. Westerhoff, S.P. Mezyk, W.J. Cooper, D. Minakata, Electron pulse radiolysis determination of hydroxyl radical rate constants with suwannee river fulvic acid and other dissolved organic matter isolates, Environ. Sci. Technol. 41(2007) 4640-4646.

[41] P. Dwibedy, G.R. Dey, D.B. Naik, K. Kishore, Rate constants for the reaction of OH radicals with some amino polycarboxylic acids, Int. J. Chem. Kinet. 32 (2000) 99-104.

[42] H. Seshadri, S. Chitra, K. Paramasivan, P.K. Sinha, Photocatalytic degradation of liquid waste containing EDTA, Desalination 232 (2008) 139-144.

[43] Y.R. Gu, W.Y. Dong, C. Luo, T.Z. Liu, Efficient reductive decomposition of perfluorooctanesulfonate in a high photon flux UV/sulfite system, Environ. Sci. Technol. 50 (2016)

10554-10561.

[44] H. Abramczyk, J. Kroh, Absorption spectrum of the solvated electron. 2. Numerical calculations of the profiles of the electron in water and methanol at 300 K, J. Phys. Chem. 95 (1991) 6155-6159.

[45] E.J. Hart, J. Boag, Absorption spectrum of the hydrated electron in water and in aqueous solutions, J. Am. Chem. Soc. 84 (1962) 4090-4095.

[46] Y. Qu, C.J. Zhang, P. Chen, Q. Zhou, W.X. Zhang, Effect of initial solution pH on photo-induced reductive decomposition of perfluorooctanoic acid, Chemosphere 107 (2014) 218-223.

[47] C.L. Thomsen, D. Madsen, S.R. Keiding, J. Thogersen, O. Christiansen, Two-photon dissociation and ionization of liquid water studied by femtosecond transient absorption spectroscopy, J. Chem. Phys. 110 (1999) 3453-3462.

[48] O. Hironobu, H.A. Masaaki, S. Ken, A photo-hydrogen-evolving molecular device driving visible-light-induced EDTA-reduction of water into molecular hydrogen, J. Am. Chem. Soc. 128 (2006) 4926-7.

[49] E. Bae, W. Choi, Effect of the anchoring group (carboxylate vs phosphonate) in Ru-complexsensitized $TiO_2$ on hydrogen production under visible light, J. Phys. Chem. B 110 (2006) 14792-14799.

[50] K. Hirano, E. Suzuki, A. Ishikawa, T. Moroi, H. Shiroishi, M. Kaneko, Sensitization of $TiO_2$ particles by dyes to achieve $H_2$ evolution by visible light, J. Photoch. Photobio. A 136 (2000), 157-161.

[51] S. Bhosale, A.L. Sisson, P. Talukdar, A. Fürstenberg, N. Banerji, E. Vauthey, G. Bollot, J. Mareda, C. Röger, F. Würthner, N. Sakai, S. Matile, Photoproduction of proton gradients with π-

stacked fluorophore scaffolds in lipid bilayers, Science 313 (2006) 84-6.

[52] N. K. Vel Leitner, I. Guilbault, B. Legube, Reactivity of •OH and $e_{aq}^-$ from electron beam irradiation of aqueous solutions of EDTA and aminopolycarboxylic acids, Radit Phys. Chem. 67 (2003) 41-49.

[53] J.J. Wang, Z.B. Guo, Y.F. Zhao, S.N. Zhu, X.Y. Shen, Y. Bai, J. Ren, Research on degradation effect and the mechanism of sulfamethoxazole under gamma-ray irradiation in aqueous solution, J. Nucl. Agr. Sci. 32 (2018) 1180-1185.

[54] M. Sun, H. Zhou, B. Xu, J.X. Bao, Distribution of perfluorinated compounds in drinking water treatment plant and reductive degradation by UV/$SO_3^{2-}$ process, Environ. Sci. Pullut. Res. 25 (2018) 7443-7453.

[55] T.-H. Kim, S.-H. Lee, H.Y. Kim, K. Doudrick, S. Yu, S. D. Kim, Decomposition of perfluorooctane sulfonate (PFOS) using a hybrid process with electron beam and chemical oxidants, Chem. Eng. J. 361 (2019) 1363-1370.

[56] C. Blondel, P. Cacciani, C. Delsart, R. Trainham, High-resolution determination of the electron affinity of fluorine and bromine using crossed ion and laser beams, Phys. Rev. A 40 (1989) 3698-3701.

[57] A. Paul, C.S. Wannere, H.F. Schaefer, Do linear-chain perfluoroalkanes bind an electron? J. Phys. Chem. A 108 (2004), 9428-9434.

[58] P.A. Babay, C.A. Emilio, R.E. Ferreyra, E.A. Gautier, R.T. Gettar, M.I. Litter, Kinetics and mechanisms of EDTA photocatalytic degradation with TiO2, Water Sci. Technol. 44 (2001) 179-185.

[59] D. Chen, A.E. Martell, D. McManus, Studies on the mechanism of chelate degradation in iron-

based, liquid redox $H_2S$ removal processes, Can. J. Chem.-Rev. Can. Chim. 73 (1995) 264-274.

## Highlights

- UV/EDTA process is effective in PFOS decomposition over a wide range of pH.
- Air has negligible effect on PFOS decomposition in UV/EDTA process.
- EDTA can scavenge •OH to protect $e_{aq}^-$.
- Prolong the survival time of $e_{aq}^-$ to increase steady-state concentration of $[e_{aq}^-]_{ss}$.